

ELMS: Elasticized Large Language Models On Mobile Devices

Wangsong Yin[◆], Rongjie Yi[◇], Daliang Xu[◆], Gang Huang[◆],
Mengwei Xu[◇], Xuanzhe Liu[◆]

[◆]Key Lab of High Confidence Software Technologies (Peking University), Beijing, China

[◇]State Key Laboratory of Networking and Switching Technology (BUPT), Beijing, China

yws@stu.pku.edu.cn

mwx@bupt.edu.cn

liuxuanzhe@pku.edu.cn

Abstract

On-device Large Language Models (LLMs) are revolutionizing mobile AI, enabling applications such as UI automation while addressing privacy concerns. Currently, the standard approach involves deploying a single, robust LLM as a universal solution for various applications, often referred to as LLM-as-a-Service (LLMaaS). However, this approach faces a significant system challenge: existing LLMs lack the flexibility to accommodate the diverse Service-Level Objectives (SLOs) regarding inference latency across different applications. To address this issue, we introduce ELMS, an on-device LLM service designed to provide elasticity in both the model and prompt dimensions of an LLMaaS. This system includes: A one-time neuron reordering technique, which utilizes the inherent permutation consistency within transformer models to create high-quality, elastic sub-models with minimal runtime switching costs. A dual-head compact language model, which efficiently refines prompts and coordinates the elastic adaptation between the model and the prompt. We have implemented this elastic on-device LLM service on several off-the-shelf (COTS) smartphones and evaluate ELMS using both standalone NLP/mobile-agent datasets and synthesized end-to-end traces. Across a range of SLOs, ELMS surpasses four strong baselines by up to 16.83% and 11.04% in absolute accuracy on average, with less than 1% Time-To-First-Token (TTFT) switching overhead, comparable memory usage, and fewer than 100 offline GPU hours.

1 Introduction

Large Language Models (LLMs) are ushering in a transformative era for mobile AI. A multitude of killer apps are built on top of LLMs, encompassing mobile UI automation [71], API-calling [23] and screen content comprehension [15]. For instance, one can easily place an order by simply saying “Order a pizza now from Pizza Hut” in smartphone.

With ever-growing privacy concerns, there is an emerging paradigm of mobile LLM deployment: local LLM as a system service, namely LLM-as-a-Service (LLMaaS) [1, 44, 47, 53, 82].

Akin to location or notification services, LLM service runs as a standalone system service in background and serves LLM requests (text in, text out) from third-party apps. Such a paradigm is completely feasible thanks to the world knowledge and in-context learning abilities of LLMs. With the OS’s visibility into the service, LLMaaS is also resource-efficient. Only one copy of LLM weights is needed in memory, preventing the device memory from being exhausted by app-specific models. With a converged model architecture and operator set, the LLM service can better enjoy the system level scheduling optimizations (e.g., batching or priority queues) and hardware accelerators (e.g., GPUs, DSPs, or NPUs). An industrial example is Google’s Android AICore [1], a built-in on-device LLM service in Android OS that has been used by apps like GBoard smart reply and Pixel voice recorder. Similar paradigm can also be found in Apple [3] and Intel [8].

Elastic on-device LLM service. We identify a crucial yet unexplored system feature of on-device LLM service — performance elasticity. Specifically, each app calling LLM service demands its own Service-Level Objective (SLO) on inference latency, yet a single static LLM cannot meet the diversified SLOs. Demand of elasticity is further exaggerated and complicated since LLM inference consists of two distinct stages: prefill (prompt processing speed) and decode (token generation speed), whose latencies are measured by Time-To-First-Token (TTFT) and Time-Per-Output-Token (TPOT), respectively. For instance, a chatbot [9] must behave both low TTFT and low TPOT to match human reading speed; a UI-automation agent [71, 84] typically requires a low TTFT and an acceptable TPOT, as TPOT can be overlapped with UI manipulations; a screen-event recorder [15] running in background only needs a tolerable TTFT/TPOT. Failing to meet an SLO leads to serious consequences: a significant degradation of user experience, or failure in the interactions between LLM agents and the environments/tools [3, 23, 84].

In a realistic LLM service with elastic feature, an app sends a prompt to the service as well as the SLO expected, and

the LLM service needs to provide the highest text generation quality without failing the SLO. Fundamentally differing from prior work that elasticize CNNs in pre-LLM era [28, 29, 31, 72], a key opportunity in our system model is that, *both model and input (prompts) dimensions of the LLM can be elasticized*. Through multi-scale LLM pruning technique [46, 60, 76], one can get a crucial subset of weights that running at different speed; similarly, through a small language model that scores the importance of each input token [38, 50, 54], one can prune the prompt into different lengths on demand. In both ways, LLM accuracy is sacrificed for faster text generation in a flexible manner. Our pilot experiments in §2.2 explore how each dimension of elasticity impacts the LLM inference latency: TTFT (often more time consuming and requires higher elasticity) is proportional to both the prompt length and the model size; TPOT is mainly proportional to the model size with the help of KV cache [41]. **Challenges.** However, designing an LLMAaaS with efficient elasticity faces the following unique challenges.

- **Costly runtime switching between elasticized models.** Elastic service has to frequently switch between the sub-models at request level, yet traditional model elastification methods (e.g. structural pruning) often ignore this switching overhead [21, 42, 46, 72]. For instance, generated by SoTA structural pruning [46], a sub-model of LLaMA-7B with 20% parameters takes 8.2s to switch to 30% on Redmi K60 Champion. The root cause is that, to utilize the deeply optimized on-device NN inference libraries and hardware throughput, the interleaved and overlapping sub-models' weights must be re-layouted to contiguous format in memory before inference (or each sub-model must be maintained an unacceptable standalone copy in memory). In LLMAaaS, this switching overhead is billed to TTFT since the switching can only be performed right after the LLMAaaS receiving a request.

- **Sensitive prompt-model orchestration strategy.** There exist multiple elastic strategies to meet an SLO, yet their output text quality could differ significantly. Exemplified with a real prompt from ARC_E dataset in Figure 5, although both elastic strategies (50%/20% prompt/model pruning vs. 20%/50% prompt model pruning) can meet the SLO, only the first strategy leads to a correct generated answer. Another instance is that with randomized strategy, the top5 API selection of Octopus dataset exhibits a 15.2% accuracy loss to the oracle strategy on an SLO with 50% TTFT and 80% TPOT of the full LLaMA-7B model. How to orchestrate the two dimensions of elastification to maximize the LLM output quality at request level has not been touched in prior study.

Our solution: ELMS. We present ELMS, a first-of-its-kind elastic on-device LLM service that tackles the above challenges through following novel techniques.

One-shot reordering of permutation consistent units (§3.2). This technique performs pruning on a fine granularity

of *permutation consistent units* in Transformers. Identified by ELMS, these units can be offline arbitrarily layouted in a block (e.g., Attention or MLP) while guarantee the equivalent input/output as original block, thereby fundamentally avoiding the runtime switching overhead. Specifically, such a unit is an entire attention head (i.e., columns in $W_Q/W_K/W_V$ and rows in W_O with the same indices), or an entire MLP neuron (i.e., a columns in W_{up} and a row in W_{down}). In the one-shot reordering, ELMS first profiles the importance of the units through an eXplainable-AI (XAI) [35, 57, 62] guided method, which measures unit importance via gradients. Then, ELMS reorders the units in memory based on their importance, making each contiguous memory segment (starting from base address to a memory pointer) a sub-model. After re-ordering by importance, the pruning always extends from the periphery inward, thus requiring no online reordering. The profiling and reordering are all done offline, incurring no online overhead. The online switching of sub-models is zero-cost by only moving the pointer. ELMS further incorporates other optimizations such as LoRA recovery and anchor layers locking to improve the sub-models quality.

Dual-head Tiny Language Model (TLM) for prompt-model elastification orchestration (§3.3). Different from prior work [38, 54] that only focus on identifying important tokens, ELMS designs a dual-head TLM as an end-to-end solution for determining an optimal prompt-model elastification strategy. Specifically, the TLM features two heads, namely score-head and decision-head. During inference, the score-head estimates the token importance, while the decision-head chooses the proper prompt- and model- elastification ratios (mapped to the real latency by a one-shot profiling on various SoCs). At offline, the decision-head learns from the prompts and groundtruth of a generic corpora. As a self-induced labelling process, all possible strategies of a prompt with its SLOs are traversed to get the inference result, and an optimal strategy is recorded as the label. Both the training and inference of TLM are cost-effective with careful optimizations like reusing the compact MobileBert and bottom layers sharing.

Evaluation. We have fully implemented ELMS on 3 COTS smartphones and 5 base/instruction-tuned LLMs with 3B–7B parameters. The datasets encompass fundamental language tasks ARC_E/OBQA [24, 49], mobile UI automation tasks LlamaTouch [84], and mobile system API-calling tasks Octopus [23]. Evaluation shows that ELMS achieves up to 16.83% and on average 11.04% higher absolute accuracy on end-to-end traces, and up to 34% and on average 22% on standalone datasets, when meeting all request SLOs. Within 2% absolute accuracy loss, ELMS can speed up TTFT by up to 5× and TPOP by up to 2×. The runtime memory consumption is also on-par with non-elastic LLM service. The entire elastification of ELMS only takes 68.3 GPU hours (within \$100 GPU renting cost [7])

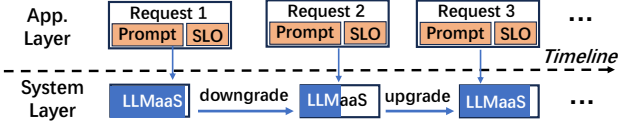


Figure 1: System model of elastic LLM service. The service can be upgraded/downgraded at runtime to adapt to various SLOs.

when elasticizing LLaMA-7B for MI14 smartphone, being affordable for most LLMaaS developers.

Contributions are listed as follows:

- We highlight the strong motivation and key challenges of elastic on-device LLM service.
- We present the first elastic LLM service, ELMS, which fully exploits the space of model and prompt elastification through two novel techniques/designs, one-shot reordering of permutation consistent units and dual-head tiny language model.
- We conduct comprehensive experiments on ELMS that demonstrate its superior performance over competitive baselines. The code will be made public after acceptance.

2 Background and Motivations

2.1 Elastic on-device LLM service

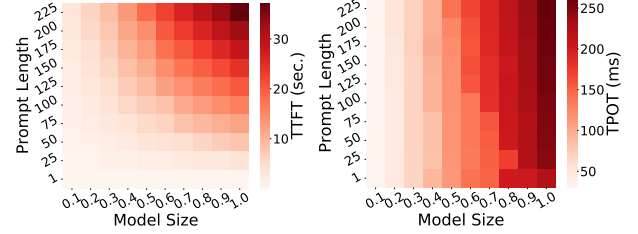
On-device LLM as a service. With ever-growing privacy concerns, recently there is a trend proposing running a single yet powerful (e.g., 7B-size) LLM as a system service (LLMaaS) on mobile devices [1, 44, 47, 53, 82]. In doing so, various apps/agents share the same LLM, minimizing the efforts and resources of preparing and managing task-specific models.

We identify a key system challenge of LLMaaS: the LLM requests from different apps or tasks have diversified SLO demands on inference latency, yet current LLMs lack the elasticity to do so. For instance, as listed in Table 1, a chatbot must behave both low TTFT and TPOT in order to match human reading speed. A UI-automation agent requires a relatively low TTFT to generate the first action and an acceptable TPOT, since the following latency can be overlapped with the manipulation of UI elements and thus transparent to users. Besides, these mobile-agents typically only decode few tokens compared to the prompt length. Failing to provide satisfactory latency for a request leads to serious consequences: a significant degradation in user experience, or failure in the interactions between LLM agents and the environment/tools.

How to satisfy the heterogeneous demands of different LLM requests, while not degrade the LLM output quality

Mobile LLM App.	Service-Level Objective
Chatbot [9]	Readable TTFT/TPOT
Always-on Voice Assistant [6, 16]	Very-Low TTFT, medium TPOT
Background Screen-Event Recorder [15]	Tolerable TTFT/TPOT
Smart Message Reply [5]	Low TTFT, low TPOT
API-Calling Agent [23]	Low TTFT, acceptable TPOT
UI-Automation Agent [71, 84]	Low TTFT, acceptable TPOT

Table 1: SLOs of various mobile LLM applications.



(a) Prefill latency.

(b) Decode latency.

Figure 2: LLM inference latency w.r.t. prompt length and model size. Measured on LLaMA-7B, Redmi K60 Champion (Snapdragon 8Gen2).

significantly? One plausible solution is to deploy a dedicated-sized LLM for each SLO¹. This is unfriendly (and even infeasible) to both the LLMaaS developers and users. On one hand, costly GPU resources are required for pretraining multiple LLMs; on the other hand, memory consumption rises dramatically in order to manage these LLMs — running counter to the motivation behind LLMaaS.

System model of elastic LLM service. Thereby, we propose a model of elastic LLM service. As illustrated in Figure 1, at system layer, there is one running LLM that serves requests from the application layer (e.g., apps/agents). Each request consists of a prompt (a text sequence as LLM input) and an SLO (inference latency constraint). This single LLM can rapidly upgrade/downgrade itself to a more bulky/swift one at runtime to adapt to a specific SLO.

2.2 Opportunities and challenges

We present several observations to show the opportunities and challenges of realizing elastic LLM service.

Observation#1: LLM inference latency is influenced by two dimensions — prompt and model. An LLM inference workload can be divided into two dimensions: prompt (activations) and model (weights). We conduct a measurement of LLaMA-7B inference on Redmi K60 Champion smartphone equipped with Snapdragon 8Gen2 SoC. We use 4 threads (big cores). The “model size” here represents a sub-model of LLaMA-7B [68] (e.g., 0.1 means 10% parameters). In Figure 2, we observe that both the two dimensions can influence LLM

¹In cloud datacenters, a tighter SLO can be achieved by scaling up hardware resources, e.g., number of GPUs/TPUs. However, hardware resource of mobile devices is limited and not scalable.

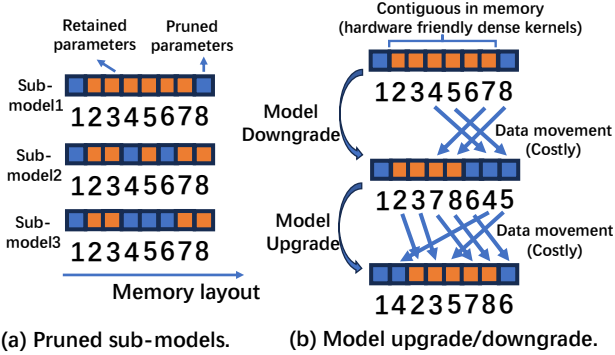


Figure 3: Elastic LLM does not translate to Elastic LLM service. Non-negligible request-level overhead of data movement is still suffered when directly employing model pruning.

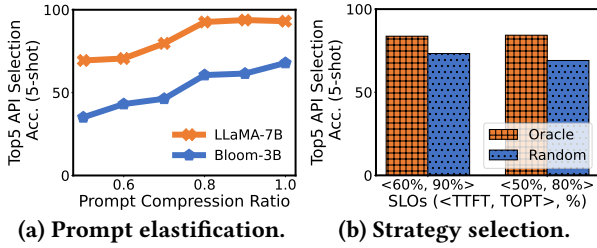


Figure 4: Prompts of on-device LLM service are also elasticizable. Yet the ratio needs careful (and content-aware) selection to achieve an optimal orchestration with model elastification.

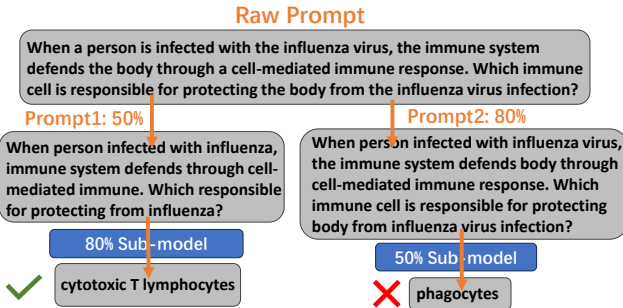


Figure 5: Sensitive prompt-model orchestration. We use a prompt of ARC_E dataset and the elasticized LLaMA-7B as an exemplification. The SLO is 40% TTFT of the full LLM.

inference latency. TTFT is influenced by both prompt length and model size; TPOT is mainly determined by model size².

²Only when the prompt is extremely long (e.g. over 10K tokens), the attention operator will dominate inference, and TPOT will then be influenced by prompt length.

We have the following proportional relationships:

$$\begin{aligned} TTFT &\propto PromptLength \times ModelSize, \\ TPOT &\propto ModelSize, \end{aligned} \quad (1)$$

Notably, as shown Figure 2, TTFT is much longer than TPOT (e.g. seconds v.s. milliseconds), which necessitates a more aggressive elastification of TTFT.

Observation#2: LLMs are elasticizable; yet elastic LLM does not necessarily translate to elastic LLM service. DNNs are known to be elasticizable: they can provide various compute-accuracy tradeoffs by a subset of their parameters (known as pruning [29, 46]). For instance, Sheared-LLaMA [76] demonstrates that pruning off 60% parameters of a 7B-size LLM can still retain 74% of original accuracy on ARC_E dataset [24]. LLMPruner [46] further shows that with lightweight Parameter-Efficient Fine-Tuning (PEFT) methods, the accuracy loss incurred by pruning could be recovered. Since pruning (and PEFT) generates sub-models that share the same superset of parameters, there is no overhead of extra memory or pre-training that mentioned in §2.1.

Yet, the challenge is that, since the model upgrades/downgrades itself to adapt to various requests' SLOs, switching between these sub-models is not overhead-free. As shown in Figure 3a, although sub-models share the same superset of parameters, they are no longer contiguous in memory. One may change the deeply optimized dense kernels of on-device NN libraries (e.g., MNN [39] or mllm [12]) to handcrafted sparse kernels. However, these kernels typically undergo degraded performance without fully exploiting the parallelism of processors (e.g., mobile GPUs/NPUs or multi-core CPUs). Another compromising method is to perform a movement of parameter data for each model switching, as shown in Figure 3b. Although the switching overhead is mitigated from iteration/operator level to request level, it is still non-negligible. For instance, movement of LLaMA-7B's a W_Q matrix (4096×4096) takes 139 ms on Redmi K60 Champion smartphone in the worst case, and consequently the entire model suffers time overhead at seconds level.

Observation#3: Prompts of on-device LLM service are also elasticizable. Intuitively, as a natural language sequence, a prompt could still preserve essential semantic information when refined to a shorter one. Especially, the prompts of LLM service callers tend to be verbosely designed in order to maximize the LLM's instruction following [52, 88] and in-context learning [26, 73] abilities. In other words, the prompt dimension can also be elasticized just like the model dimension. We showcase employing a commonly used prompt compression method LLMingua2 [54] for Octopus [23] dataset, which contains traces of an on-device API-calling agent. LLMingua2 identifies and preserves most semantically significant tokens by a dedicated language model. We report

top5 function match accuracy of Octopus. As shown in Figure 4a, the accuracy shows a well-performing tradeoff curve when gradually compressing the prompt.

However, the challenge is the sensitive prompt-model orchestration. An intuitive example is that, if a request sets its SLO as 40% TTFT and 80% TPOT³, we cannot know which strategy is golden a priori — a 50% prompt with an 80% model? an 80% prompt with a 50% model? or others?⁴ Prompts with various content naturally require distinct and customized strategies. In Figure 4b and Figure 5, we demonstrate that a strategy without careful design (e.g., random) may lead to a significant degradation on accuracy. We use LLaMA-7B elasticized by our method (elaborated in §3.2) on Octopus dataset. The prompt is elasticized by LLMlingua2.

Implications. On-device LLM service exhibits opportunities and challenges of being elasticized through prompt and model. In response, we present ELMS, an end-to-end elastic LLM service that orchestrates these two dimensions to provide latency-centric service.

3 ELMS Design

3.1 Overview

Design goal. ELMS aims to provide LLM service that adapts to a specific Service Level Objective (SLO) of resource constraint per request (prompt), while maximizing the service quality (i.e., LLM generation accuracy).

SLO definition. In this paper, we define SLO of LLM service as a tuple $\langle \zeta_{TTFT}, \zeta_{TPOT} \rangle$, where ζ is the compression ratio to full LLMAaaS latency. The SLOs that an LLMAaaS should serve is pre-defined by the service developers.

Workflow. ELMS's idea is to orchestrate model- and prompt-level elastification, both of which need offline preparation. To achieve this, its workflow is designed as a cloud, offline stage and a device, online stage, as shown in Figure 6.

At cloud offline stage, on one hand, the model is elasticized to various levels of sub-models that share the memory and can be cost-effectively switched (§3.2). On the other hand, we on-cloud fine-tune a TLM for prompt elastification (§3.3).

At device online stage, the elasticized LLM and fine-tuned TLM are deployed on mobile devices as a service. For each LLM service request, the prompt and the corresponding SLO are fed into the fine-tuned TLM. The TLM then outputs a compressed prompt and selects a sub-model with proper size. Finally, an LLM inference that satisfies the given SLO is performed atop the sub-model and the compressed prompt.

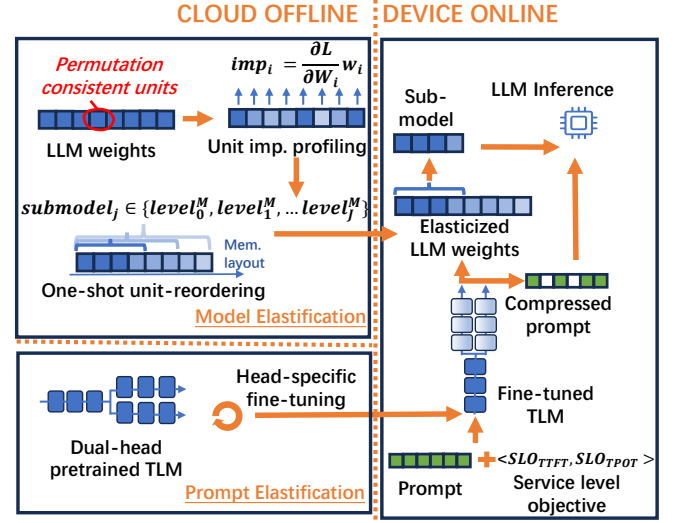


Figure 6: Workflow of ELMS.

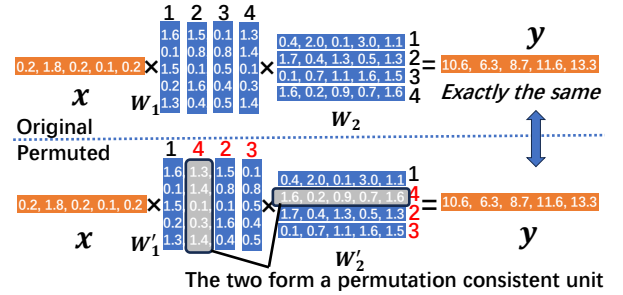


Figure 7: Illustration of permutation consistency.

3.2 Model elastification

Permutation consistent units of Transformer models. We explore a mathematically provable characteristic of Transformer models — permutation consistency.

Property 1. Units of a neuron network are called permutation consistent units if they can be reordered between each other in a block without affecting the block's input/output.

This property indicates that a dense operator kernel can equivalently process these units in arbitrary order without any runtime data re-layout. The rationale behind it is that the Reduce operator (e.g., sum/min/max) satisfies the commutative and associative laws. A basic block that contains such units is $y = xW_1W_2$ in Figure 7. Its permutation consistent unit is a column of W_1 together with the corresponding row of W_2 . If we permute the weights as shown in Figure 7, the intermediate activation xW_1' will be permuted in response. Nevertheless, W_2' is also permuted in the same order, so the multiplication of MatMul operator can still be performed correctly. Since the following addition of MatMul operator is a Reduce operator, the calculated $xW_1'W_2'$ is exactly the same

³See our formal definition of SLO in §3.1.

⁴According to formula 1, there are multiple combinations of prompt and model that can meet the exemplified SLO.

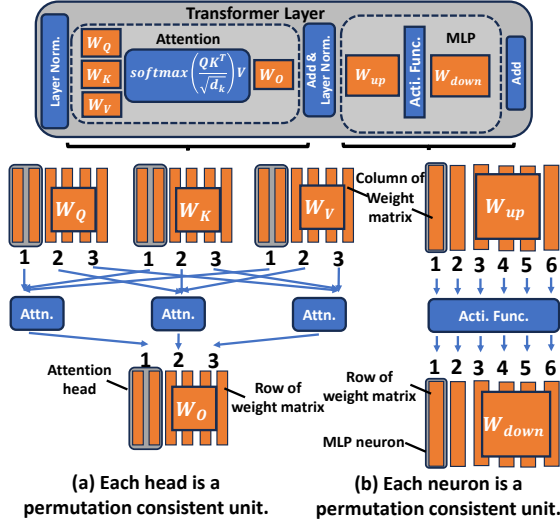


Figure 8: Permutation consistent units in Transformer.

as xW_1W_2 . Notably, different from prior work [87] that also leverages the Reduce operator to permute DNNs, ELMS’s key insight is to identify such a joint unit in two-layer blocks that are ubiquitous in Transformers. Permutation of this unit can be made completely offline, while [87] still needs online reordering the input with a single operator level abstraction.

Property 2. Attention heads and MLP neurons of Transformer models are permutation consistent units.

As shown in Figure 8, there are two types of permutation consistent units in the main weights of a Transformer layer, i.e., attention heads and MLP neurons, and they are independent to each other. Specifically, the contiguous columns/rows with the same indices in W_Q, W_K, W_V and W_O (i.e., an attention head) constitute a permutation consistent unit; a column/row with the same index in W_{up} and W_{down} (i.e., an MLP neuron) also constitute a permutation consistent unit. The derivation process is similar to the example in Property 1, Figure 7 — the last operator of attention and MLP blocks is Reduce. Property 2 holds true for mainstream Transformer-based language models with variants like RoPE⁵ [59], biased QKV [20], GQA [27] or gated MLP [68].

Our method: one-shot unit-reordering. Based on Property 1 and Property 2, we propose a novel model elastification method as shown in Figure 9. Its key idea is to “atomize” the Transformer into the units shown in Figure 8, and then group them to construct a series of sub-models that each is contiguous in memory.

• *Offline.* Specifically, ELMS first profiles importance of each unit offline (detailed later). Since these units are permutation

consistent, ELMS freely reorders them by their importance in descending order (if importance is the higher the better), starting from the base address of the weight tensor. Notably, the reordering is only performed intra-block, e.g., reordering the unit of attention heads in the same attention block. Then, ELMS groups these units into sub-models. For example, in Figure 9, sub-model in $level_3^M$ contains units with indices (not address) “1 5 8 2”, and sub-model in $level_1^M$ contains “1 5 8 2 3 4 7”. The sub-model sizes and numbers $\{level_1^M, \dots, level_J^M\}$ are pre-defined by the LLMAaaS developers. In practice, we set this to a fine enough granularity (a global ratio of 20% to 100% in a step size of 10%, by default). Such a ratio is evenly shared by all Transformer layers that need elastification. After that, low-rank adapters [34] are attached to each sub-model to recover potential generation quality loss (if there is any) of these sub-models. We elaborate such a recovery process in the following parts. So far, the LLM weights have been elasticized into a series of high-quality sub-models that run in various speed. We demonstrate the quality of generated sub-models in Figure 10a.

• *Online.* In Figure 9b, the upgrading of model is performed in the following steps: ELMS first detaches the corresponding adapter from sub-model $level_1^M$, which has served the last request. Then, it moves the ending memory pointer of the weights tensor from the address of unit with index “2” to “7”. After that, ELMS attaches another adapter to sub-model $level_3^M$, and the upgrading is finished. Such a process is very cost-effective on mobile devices — it does not involve any data movement compared to traditional pruning methods, and can still utilize deeply-optimized dense kernels provided by NN libraries. For instance, upgrading W_Q to 4096×4096 size only takes 2 ms on Redmi K60 Champion smartphone, while a naive pruning method must undergo a 140ms data movement.

Profiling unit importance through explainable-AI. Parameters of neuron networks are known to feature diverse importance. For instance, a weight element with higher magnitude may contribute more to NN capability [32, 36, 43]. Inspired by the concept of eXplainable-AI (XAI) [35, 57, 62], ELMS profiles unit importance with a more accurate method, i.e., by the next-token prediction loss function L on a calibration corpus C . The intuition behind XAI is that, if a unit is more important, it should make L larger on C when been removed. Specifically, we define importance of unit i as $imp_i = |L - L_{W_i=0}|$. By Maclaurin series [63], we get

$$imp_i = |L - L_{W_i=0}| = \left| \frac{\partial L}{\partial W_i} W_i + o(\|W_i\|^2) \right|. \quad (2)$$

Since the second term is a higher-order infinitesimal, ELMS then takes $|\frac{\partial L}{\partial W_i} W_i|$ as a estimation of unit importance. By default, C is set to a sub-set of bookcorpus [89], which is a general-purpose language-modeling dataset.

⁵RoPE only introduces position information in sequence axis and intra-head axis.

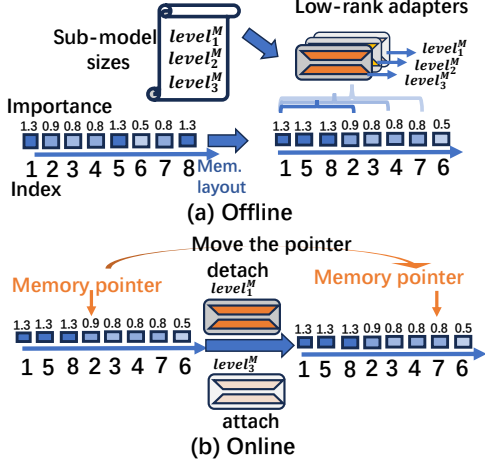


Figure 9: ELMS offline profiles and reorders permutation consistent units in one-shot; it online switches (i.e., upgrade/downgrade) sub-models by cost-effectively attaching/detaching the corresponding adapters and moving the memory pointer.

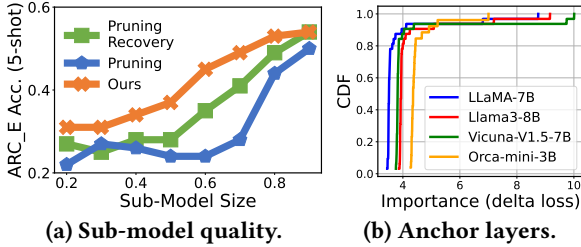


Figure 10: (a) ELMS generates sub-models that with consistently higher quality than pruning and pruning+recovery [46]. (b) A small portion of layers, i.e., ‘anchor layers’, is much more important than others.

Besides, interestingly, we find that several layers are much more important than other layers. We call these layers ‘anchor layers’. We measure the importance of a layer by the increase of loss function when a layer is removed. As shown in Figure 10b, the importance of layers exhibits a power-law distribution (80/20 rule), which means about 20% layers are anchor layers. As a result, we lock these layers from elastification. For example, if we need a 50%-size sub-model of a 32 layers LLM, we retain 37.5% permutation consistent units for each non-anchor layer (26 layers in total).

Task-agnostic low-rank recovery of sub-models. We add Low-Rank Adapters (LoRAs) [34] to the frozen $W_{Q/K/V/O}$ and $W_{up/down}$ of each sub-model to recover them from potential accuracy loss. A LoRA is two low-rank matrices $A \in \mathbb{R}^{n \times r}$ and $B \in \mathbb{R}^{r \times m}$ that trained as a side branch of main weights. ELMS’s default setting of r is 8, an empirically common practice in LoRA-based tunings. LoRA weights are only 0.1%–0.5%

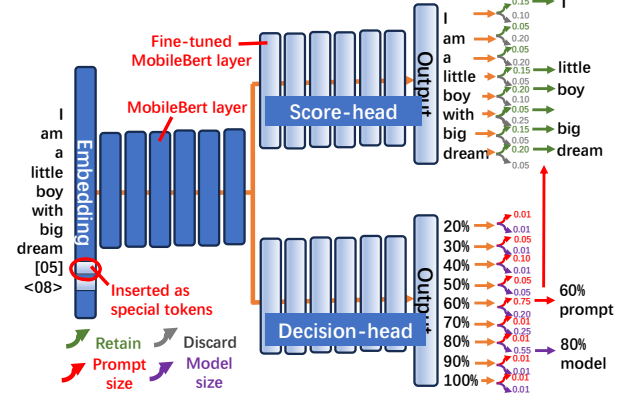


Figure 11: The dual-head TLM.

of the entire LLM weights, and thus such a method only introduces <5% extra memory overhead even under ELMS’s fine-grained sub-model settings. The switching overhead is also minimized since the attaching/detaching operations are all low-rank MatMul and element-wise MatAdd.

Different from traditional language models that need tuning on specific downstream tasks (e.g., Bert [25], T5 [56]), LLM commonly serves as a generic task solver. Thereby, ELMS’s sub-model recovery is *task-agnostic*. LoRAs are trained with next-token prediction loss that identical to the pre-training process. Thanks to LoRA’s preservation of the LLM backbone’s capability, a general, high-quality and moderate-size corpus can handle this recovery well. By default, each sub-model is recovered on about 50M tokens of Alpaca-cleaned [2, 65] dataset. We also discuss the impact of recovery data in §5.5.

Remarks ELMS’s model elastification generates fine-grained, high-quality sub-models with both acceptable offline overhead and negligible online overhead.

3.3 Prompt elastification

Dual-head TLM. ELMS tackles the challenges mentioned in §2.2 by a dual-head Tiny Language Model (TLM). As shown in Figure 11, the TLM is a variant of mobile-friendly pre-trained language model MobileBert [61], a compact model with only 20% parameters of BERT_base [25] yet just 0.7% accuracy loss on GLUE benchmark [69]. We make the following modifications. Firstly, the SLO of the current request is marked in natural language and inserted into the embedding layer of MobileBert as special tokens. For instance, “[05]” represents the prefill SLO is 50% TTFT; “<08>” is 80% TPOT. These special tokens are initialized to word vectors that orthogonal to each other. Secondly, the TLM is designed with two separate heads, named score-head and decision-head. The score-head treats each token of the prompt as a two-class classification problem, where each token can be classified

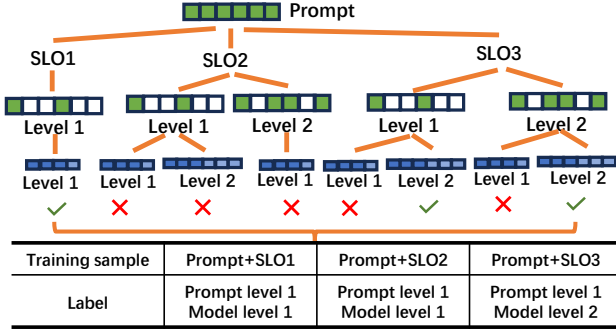


Figure 12: Illustration of the self-induced labelling process of decision-head training data collection.

into “discard” or “retain”. The decision-head treats the entire sequence of prompt with SLO as two multi-class classification problems. Each possible model elastification level (i.e., the sub-model size, discussed in §3.2) is a class of one problem; possible prompt elastification levels are classes of the other problem. Akin to model elastification, the prompt is also pre-defined to multiple fine-grained levels that denoted $\{level_1^p, \dots, level_k^p\}$ by the LLMAaaS developers. By default, we set it in alignment with model elastification levels. Besides, the two heads share the same bottom layers (12 out of 24 layers by default) based on the rationale that bottom layers of DNNs are mainly responsible for capturing basic instead of task-specific information. In doing so, the overhead of TLM inference/training is further minimized.

TLM inference. At decision-head, ELMS takes the class with the max probability as its decision. For example, in Figure 11, the decision-head selects a 60% prompt and 80% model. At score-head, ELMS ranks the prompt tokens by the probability of “retain”, then selects top ones according to decision-head. Notably, if the TLM outputs a decision that cannot meet the SLO (which is nearly yet not impossible due to the black-box property of DNNs), ELMS will execute a runtime check and the decision will fall back to a random one that stringently meet the SLO. After inference, we get a compressed prompt and a selected sub-model.

The inference overhead is acceptable. Its total parameters are about 40M, which means 2 orders of magnitude less memory footprint than the LLM service. Regarding to latency, the TLM can still perform an on-device inference within 5% of the original LLM’s TTFT even if the LLM’s prompt is compressed while TLM’s not.

TLM training. The TLM is initialized from the pre-trained weights of MobileBert; each head is further fine-tuned individually. We keep the pre-trained embedding layer and bottom layers frozen. When training one head, the other head is also frozen.

• **Score-head.** We first use MeetingBank [11] dataset to fine-tune the score-head. The dataset contains about 50M tokens

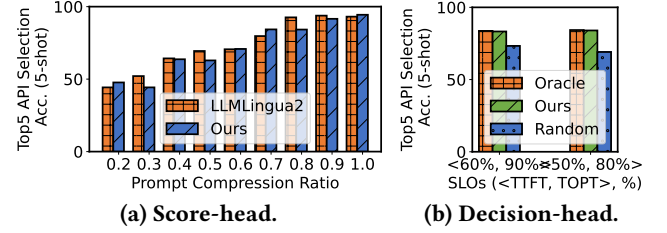


Figure 13: Effectiveness of dual-head TLM.

of corpus that each token is labelled “discard” or “retain” by GPT-4 [18]. Note that the training of score-head is independent to the decision-head and the LLM. Figure 13a shows the effectiveness of score-head with LLaMA-7B and Octopus dataset. Our method achieves on-par prompt refining ability compared to LLMlingua2.

• **Decision-head.** After training score-head, we train decision-head with the assistance of both the elasticized LLM and the score-head. The intuition is that we can traverse the decision space and learn the optimal one offline. Specifically, the training data is collected by a self-induced labelling process. In Figure 12, we provide an illustrative example. For each prompt and SLO (pre-defined by LLMAaaS developer, see §3.1), we enumerate all its possible⁶ decisions, and label it with *the most lightweight one under which the LLM can output correct answer*. If all possible decisions fail, the decision is assigned to a default one (e.g., random). By default, ELMS collects training samples from a comprehensive benchmark MMLU-Pro [70], which contains 17 domains of question-answer pairs. In Figure 13b, the decision head demonstrates significantly higher quality than random decision, and approaches oracle. We also discuss the impact of TLM training data in §5.5.

Remarks ELMS’s prompt elastification efficiently and effectively elasticizes prompt and orchestrates model- and prompt-dimension of elastic LLMAaaS.

4 Implementation

Offline stage. We build the elasticized LLM and the TLM on top of Pytorch [55]. We modify the modeling.py of Huggingface Transformers⁷ [74] library to identify the permutation consistent units and profile their importance. In doing so, ELMS can easily be made forward-compatible with LLMs released in the future. The offline elastification is performed on a cloud server equipped with 8 NVIDIA A40 GPUs.

On-device LLMAaaS. We build an LLM service on top of mllm⁸ [12], which is a lightweight yet powerful on-device

⁶The LLMAaaS developers pre-execute a one-shot profiling on a testing device within 1 hour under the guidance of Formula 1 and leverage the profiled data to judge whether a decision can meet a SLO.

⁷Commit hash c31473ed4492fdf26aec4173451f31590021862f

⁸Commit hash ed766fae54d9f1bf2b6b25018e6cc434ce223303

Name	SoC	RAM
Redmi K60 Champion Edition [13]	Snapdragon 8gen2	19GB
Mi 14 [17]	Snapdragon 8gen3	22GB
Redmi K70 Pro [14]	Snapdragon 8gen3	24GB

Table 2: Devices we use in our experiments.

LLM inference library written in pure C++ and assembly language. We pack the LLM inference program as a standalone binary file and run it as an independent process. The apps interact with it through interfaces like `bindLLMService()` and `callLLM()`. To facilitate the upgrade/downgrade of elasticized sub-models without incurring inference-time performance degradation, the `Linear` is replaced by `ElasticLinear`. Specifically, we wrap the original dense kernel with an additional memory pointer that specifies the addresses of sub-model weights. We optimize the low-rank `MatMul` and `MatAdd` of LoRA with ARM NEON [4]. The LLMAaaS runs on Commercial Off-The-Shelf (COTS) smartphones.

5 Evaluation

5.1 Experimental settings

Testbed. We conduct experiments on the following testbeds. On cloud, we use a server with a 64-core CPU (750GB RAM) and 8 A40 GPUs (45GB HBM each). On device, we test ELMS across COTS smartphones listed in Table 2.

Models. We test the following LLMs. (1) *Two base LLMs*: LLaMA-7B [68] and Llama3-8B [27]. (2) *Two instruction-tuned LLMs*: Vicuna-V1.5-7B [86] and Llama3-instruct-8B [27]. (3) *One sub-7b LLM*: Orca-mini-3B [51].

SLOs. We randomly set 6 SLOs based on a stepwise sensitivity hierarchy as shown in Table 3. We also enumerate more SLOs in Figure 19b as supplementary experiments.

LLMAaaS workload. We evaluate ELMS on both standalone datasets and end-to-end synthesized traces.

•**Datasets.** We select 4 representative datasets/benchmarks for on-device LLM evaluation: (1) ARC_E [24], a commonly used dataset for science knowledge QA and reasoning. (2) OBQA [49], a dataset for natural language and commonsense knowledge comprehension. (3) Octopus [23], an on-device API-calling benchmark that follows the natural language instruction of users and selects the most suitable functions. (4) LlamaTouch [84], a realistic and complicated on-device UI-automation agent benchmark that manipulates mobile apps following user instructions. Each entry is augmented by in-context learning in 5-shots. We report option select accuracy of ARC_E and OBQA, top-5 function (without parameters) selection accuracy of Octopus, and app invocation accuracy of LlamaTouch.

•**End-to-end traces.** We further synthesize end-to-end traces on top of the above datasets. In Table 3, we list 6 conceived apps in response to the pre-defined SLOs. The requests and

Apps	SLO	Dataset	Apps	SLO	Dataset
Rewind	<100%, 100%>	OBQA	Shortcuts	<40%, 70%>	LTouch
GMail	<80%, 90%>	ARC_E	Gboard	<20%, 60%>	OBQA
Octopus	<60%, 80%>	Octopus	XiaoAi	<20%, 50%>	ARC_E

Table 3: Apps, SLOs and datasets for trace synthesis.

groundtruths of an app are synthesized from a dataset in similar domain, since there is no public available user data in the wild. Specifically, we collect 600 entries of requests in total for a trace. To comprehensively evaluate ELMS, we emulate the distribution skewness of requests by $Num(i) = \frac{600 \times e^{\alpha i}}{\sum_{k=1}^6 e^{\alpha k}}$, where $Num(i)$ is an app’s # of request, i is the SLO level (the lower, the tighter), and α is a controlling factor. The larger the value of α , the greater the proportion of more relaxed SLOs in the trace. When $\alpha = 0$, all SLOs are evenly distributed in the trace. We synthesize multiple traces with various distributions. For each trace, we randomly shuffle the requests and set the arrival timestamp by a Poisson distribution.

ELMS configurations. The training/fine-tuning/calibration data, elastification levels and TLM configuration are the same as those described in §3.

Baselines. We compare ELMS to the following alternatives. (1) Directly employing pre-trained from scratch LLMs (PFS) for diverse SLOs is a strong yet plausible baseline. Due to the unaffordable GPU resource consumption, we select the off-the-shelf OPT [85] family. As far as we know, it provides the richest variants with fewer than 7B parameters (5 models from 125M to 6.7B). (2) LLMPruner [46] (LPruner) is a State-of-The-Art (SoTA) parameter pruning method for elastification. (3) Layer-wise elastification [10] (LE) prunes parameters at layer level. (4) LLMlingua2 [54] + Contextual sparsity [45] (LG2+CS) compresses prompts at prefill stage, and dynamically activates MLP neurons for each token at decode stage.

5.2 End-to-end performance

We first evaluate end-to-end performance on traces in §5.1.

Accuracy. We report the request-response accuracy when all requests’ SLOs are met in a trace. We compare the correctness of the LLM’s answer to groundtruth. We set three levels of trace skewness: $\alpha = 0$ (even), $\alpha = 0.25$ (towards relaxed) and $\alpha = -0.25$ (towards tight). Each trace is executed on three diverse COTS devices listed in Table 2. The results are averaged across these three devices and shown in Figure 14.

ELMS significantly outperforms the baselines by 6.00%–16.83% (11.04% on average) in absolute accuracy. Compared to PFS, ELMS further involves prompt elastification and does not introduce costly switching overhead. Besides, PFS does not fully make use of the room below a given SLO. Another potential reason is that ELMS derives sub-models from a bulky one, which may feature stronger emergent ability than the

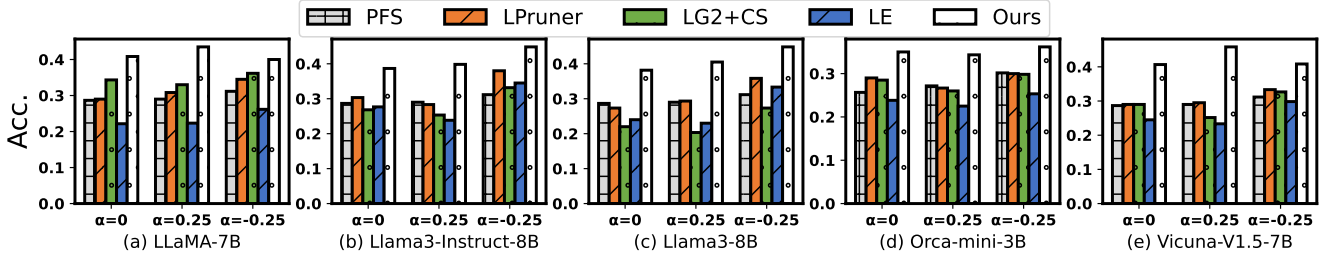
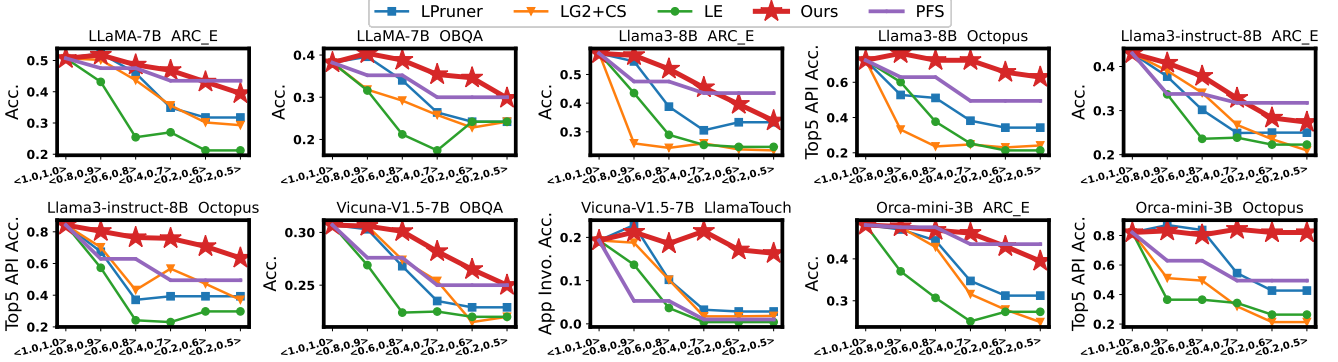
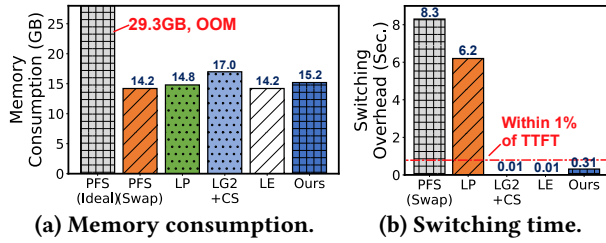
Figure 14: End-to-end request-response accuracy on the traces. α controls the SLO distribution.

Figure 15: Performance under one SLO on an entire standalone dataset without considering switching overhead.

(a) Memory consumption. (b) Switching time.
Figure 16: Online overhead. “LP” means LPruner.

SLMs pretrained from scratch. Compared to LPruner, ELMS involves prompt elastification, and minimizes switching overhead. Compared to LE, ELMS employs fine-grained permutation consistent units instead of the coarse-grained entire layers for elastification. Although both ELMS and LG2+CS orchestrate prompt- and model- elastification, there are many essential issues that degrade the performance of LG2+CS. Firstly, the heavy SLM of LLMingua2 must compress the prompt very aggressively to meet a tight TTFT SLO since contextual sparsity shows limited acceleration on prefill stage due to the low locality. Secondly, the sparsity ratio is also compromised due to non-relu [19, 68] activation functions, non-elastictizable attention [45] and degraded performance of sparse kernels.

Memory consumption. We discuss peak memory consumption in Figure 16a. Without loss of representativeness, we report LLaMA-7B in the trace with $\alpha = 0$ on Redmi K60 Champion. ELMS consumes on-par memory compared to the

baselines (15–17GB). Notably, directly deploying all the dedicated size LLMs in memory is impractical. As marked as PFS (Ideal) in Figure 16a, it consumes 29.3GB memory in total, which is OOM on all the COTS devices in Table 2.

Switching overhead. With the same setting, we report the breakdown latency of switching between different model elastification levels (i.e., sub-models) in Figure 16b. Switching time is actually part of TTFT, and a too long switching time will preempt the room of model/prompt capacity, leading to a lower accuracy. PFS (Swap) and LPruner incur unacceptable time overhead that up to 8.3/6.2 seconds per request. This is mainly attributed to the costly swapping and in-memory data movement. ELMS only takes 0.31 second to switch to a new sub-model. Such a number is lower than 1% of LLMAas’s average TTFT, thus being completely acceptable.

Remarks ELMS is the most high-quality and feasible solution for end-to-end on-device elastic LLM service.

5.3 Performance on standalone datasets

With a specific SLO, we further report the performance on an entire standalone dataset to show ELMS’s superiority. The switching overhead is dismissed as there is no upgrade/-downgrade. The results are obtained on cloud server with SLO statistics on Mi 14 smartphone, and are shown in Figure 15. We have the following observations. ELMS significantly outperforms all its baselines by up to 34% and on-average 22% on accuracy. Specifically, on all the SLOs, ELMS

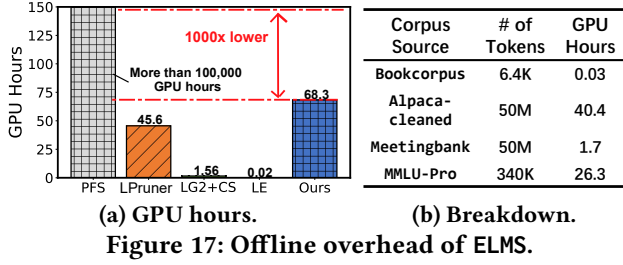


Figure 17: Offline overhead of ELMS.

always provides a much higher accuracy than the baselines (LE/LG2+CS/LPruner) that derive sub-models from the original one. Compared to PFS, ELMS provides a higher accuracy on 88.4% of all SLOs, and the maximal accuracy loss is within 9.6%. The reasons are as discussed before. Please also note that PFS is costly in terms of switching and memory at runtime.

5.4 Offline stage overhead

We further analysis the offline overhead in Figure 17. We measure the elastification of LLaMA-7B for MI14 on our A40 cloud server. Compared to PFS that trains a dedicated LLM for each SLO, ELMS derives elasticized LLMs from the original LLaMA-7B. Thereby, as shown in Figure 17a, the entire offline stage of ELMS only consumes 68.3 GPU hours (translates to about \$100 GPU renting price [7]), making it affordable for most LLMaaS developers. Compared to other baselines that also derive elasticized LLMs from the original one, ELMS takes 21.7–68.2 more GPU hours, which is acceptable since the offline stage is performed once for all. Note that in the above sections, we have demonstrated that ELMS delivers an elastic LLM service with much higher quality than these baselines.

In Figure 17b, we provide a detailed breakdown of ELMS’s offline stage. The model recovery (§3.2) and self-induced labelling (§3.3) dominate the offline stage, taking 40.4/26.3 hours. The reason the latter requires tremendous time is due to the lower GPU utilization caused by interactions with the score-head and sub-models.

5.5 Sensitivity analysis

Data sensitivity. As shown in Figure 18, the data scale of elastification exhibits a *marginal effect*. Regarding to model recovery, we further collect training data from LaMini [75] dataset that akin to Alpaca-cleaned. The final accuracy only increases 2.9%/3.7% when the recovery corpus is 10×/20× larger. Regarding to unit importance profiling and decision training data, we expand them from Bookcorpus and MMLU [33], respectively. We also observe the similar marginal effect. Since Meetingbank is currently the largest corpus for token importance scoring to the best of our knowledge, we leave expanding it as a further work. In a nutshell, ELMS’s data scale achieves a strong and sweet spot for high-quality elastification.

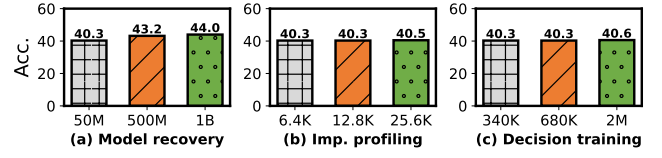


Figure 18: Data sensitivity. On trace $\alpha = 0$, LLaMA-7B.

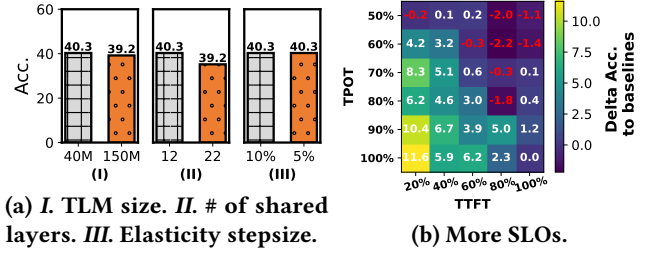


Figure 19: Configuration sensitivity.

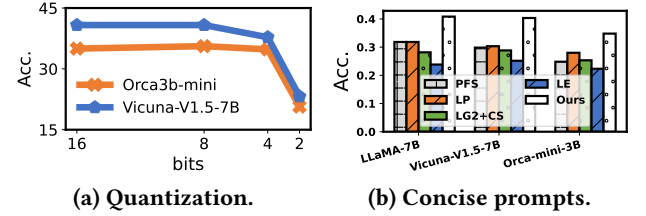
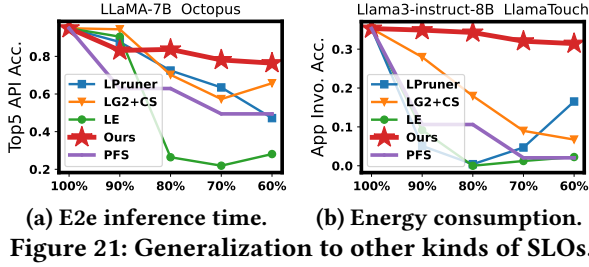


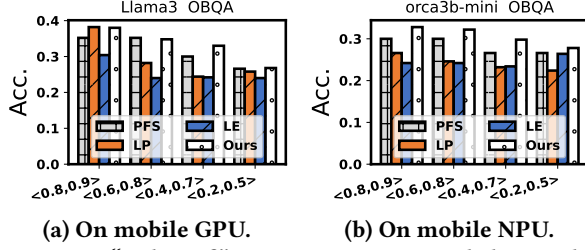
Figure 20: Model quantization and prompt conciseness.

Configuration sensitivity. We discuss the sensitivity of ELMS’s configurations in Figure 19. In Figure 19a, we use the trace of $\alpha = 0$ on LLaMA-7B. We have the following conclusions. (1) 40M parameters are already a sweet config. of TLM scale. A larger TLM’s gain on scoring and decision-making accuracy quickly gets eliminated by the overhead. (2) 12 shared bottom layers are reasonable for TLM, since more will lead to a smaller capacity of the heads, and less will incur a higher inference/training overhead. (3) A step size of 10% for model and prompt elastification is fine-grained enough for serving the diversified SLOs. Shrinking it to 5% makes almost no difference. We also provide a more comprehensive SLO configuration in Figure 19b and report the delta accuracy of ELMS compared to its strongest baseline PFS (without considering switching overhead) on ARC_E LLaMA-7B. ELMS is close to or much better than PFS on all SLOs, especially those that have a much more tighter TTFT and are more common on mobile LLM tasks. In end-to-end traces, ELMS can even achieve a better performance with its overhead-free switching.

Quantization. Quantization is a widely-used technique for deploying LLMs on mobile devices. Here we employ a linear and weights only method on the $\alpha = 0$ trace in Figure 20a. ELMS can deliver LLM service with almost lossless accuracy under 8bits integers, and acceptable (3% lower absolute accuracy) under 4bits.



(a) E2e inference time. (b) Energy consumption.
Figure 21: Generalization to other kinds of SLOs.



(a) On mobile GPU. (b) On mobile NPU.
Figure 22: “What if” experiment on mobile accelerators that cannot seamlessly run ELMS and its baselines currently. LG2+CS is omitted due to its sparse compute.

Concise prompts. We further emulate the scenario where the prompts have been consciously streamlined by the LL-MaaS callers. We use LLMingua2 to filter out about 15% verbose tokens in the prompt. The results (on trace with $\alpha=0$) in Figure 20b show that ELMS can still significantly outperform its baselines.

5.6 Generalization to other SLOs

Although in this paper we identify LLM inference latency as the SLO of LLMAaaS requests, the SLO can also be easily generalized to other metrics with our proposed elastification methods. Here we define another two SLOs: end-to-end request inference time SLO_{time} (i.e., prefill + decode stage) and inference energy consumption SLO_{energy} , each of which is with a step size of 10% full LLMAaaS. The results are obtained on Mi 14 smartphone. As shown in Figure 21, ELMS consistently outperforms its baselines on these new SLOs. the rationale is that these SLOs are all a specific kind of resource requirement and can be break down into prompt- and model- level elastifications. We believe that ELMS can serve various metrics of SLOs for diverse apps’ requirements.

5.7 On mobile SoC accelerators

Mobile devices (smartphones) are typically equipped with hardware accelerators (e.g., Adreno GPUs or Qualcomm NPUs) in their SoCs. These SIMD/SIMT DSAs achieve higher throughput and lower latency on traditional on-device DNNs, especially CNNs. Yet, to the best of our knowledge currently (Aug., 2024) none of them can seamlessly run prefill and decode of ELMS and all its baselines due to legacy SD-K/hardware issues like dynamic shape, graph building or

non-sparse kernels. Thus, we conduct a “what if” experiment by mapping the theoretical compute/memory load to the profiled latency on these processors. We use MNN [39] and mllm-NPU [78] for GPU/NPU profiling on Mi 14, respectively. The results are shown in Figure 22. ELMS can still significantly outperform the baselines under this setting. We believe that ELMS will become more friendly and practical to practitioners with the maturity of accelerators.

6 Related Work

Elastic neuron networks. Elastic neuron networks can change their capacity at runtime to dynamically adapt to various resource/accuracy constraints. Early exit networks [64, 67] only perform inference on bottom layers since they are empirically more critical. Yet, early exit is not suitable for elastic LLM service. On one hand, due to LLMs’ autoregressive inference nature, a skipped layer’s KV cache may be accessed later. On the other hand, using layers as the granularity for trade-offs is not fine-grained enough. Parameter sharing networks [28, 31, 72] generate memory-efficient sub-models that shares parameters with each other. For instance, NestDNN [28] and LegoDNN [31] create sub-models of CNNs via offline re-pretraining, which is costly for foundation models. Adaptivenet [72] employs a CNN-oriented supernet, which provides diverse accuracy-latency trade-offs yet needs extensive pre-training and memory resources. Activation sparsity [22, 40, 45, 58] elasticizes DNNs via sparsifying weights according to the NN inputs. An accuracy-latency trade-off can be achieved by setting the proportion of activated weights. Yet, they either focus on CNNs with relu [19] structure (e.g., convrelu++ [40], seernet [22]), or only accelerates the decoding stage of relu-based MLPs of LLMs. The LLM prefill stage cannot be elasticized due to the low locality. And the trade-off on decode stage is limited by both the sparse kernels and the attention module. Besides, the non-relu LLMs (e.g., LLaMA [68], Vicuna [86]) exhibit a poor performance without resource-extensive pre-training. In a nutshell, ELMS outperforms the above work by employing an orchestrated prompt-model elastification, providing a high-quality accuracy-latency trade-off in both TTFT and TPOT for LLMAaaS apps.

Efficient on-device LLM inference. Tremendous work [12, 39, 66, 77, 79–81] shed light on resource-efficiently deploying LLMs on mobile devices. For instance, MLC-LLM [66] is an NN-compiler with operator- and kernel- level optimizations for mobile devices. MNN [39] and mllm [12] are on-device inference libraries for LLMs. PowerinferV2 [80] addresses the memory issue of mobile devices by introducing swapping and activation sparsity to LLM inference. Targeting at elastic LLM service, ELMS is orthogonal to these work, and can benefit from them to realize the vision of on-device LLMAaaS.

Foundation models as a service. As a general task solver, or so-called “AGI”, a single foundation model is deployed as a service to process heterogeneous tasks [30, 82, 83]. For instance, AIOS [30] is a system where a single LLM runs as the “brain” to serve all apps on the device. ELMS makes it more practical on resource-constrained mobile devices.

Model collaboration. ELMS employs a dual-head tiny language model to elasticize the prompt of the LLM. Using a small model to collaborate with the big model is common in ML systems. For instance, speculative decoding [48, 77] accelerates the decode stage with a draft SLM. However, the prefill stage cannot be accelerated since it is typically compute-bound. LLMingua [37] use an SLM to refine the LLM prompt, which has several untackled issues for elastic LLM service as discussed in this paper. ELMS’s TLM is effective an efficient for elastic on-device LLMaaS.

7 Conclusion

This work has proposed ELMS, the first-of-its-kind elastic on-device LLM service that serves apps with diverse SLOs. ELMS incorporates two novel designs, i.e., one-shot reordering of permutation consistent units and dual-head tiny language model to fully unleash the potential of model- and prompt-elastification. ELMS significantly outperforms competitive baselines by up to 16.83% and 11.04% on average in accuracy.

References

- [1] 2024. AICore. <https://developer.android.com/ml/aicore>.
- [2] 2024. alpaca cleaned. <https://huggingface.co/datasets/yahma/alpaca-cleaned>.
- [3] 2024. Apple Intelligence. <https://www.apple.com/apple-intelligence/>.
- [4] 2024. ARM NEON. <https://developer.arm.com/Architectures/Neon>.
- [5] 2024. Gboard Smart Reply. <https://developers.google.com/ml-kit/language/smart-reply>.
- [6] 2024. Hey Siri: An On-device DNN-powered Voice Trigger for Apple’s Personal Assistant. <https://machinelearning.apple.com/research/hey-siri>.
- [7] 2024. Huggingface GPU pricing. <https://huggingface.co/pricing>.
- [8] 2024. Intel AI PC. <https://www.intel.com/content/www/us/en/products/docs/processors/core-ultra/ai-pc.html>.
- [9] 2024. Llama.cpp. <https://github.com/gganganov/llama.cpp>.
- [10] 2024. LLM layer pruning. https://github.com/horseee/LLM-Pruner/blob/cbe48894ed772f342e99d3d0efbab9df6520c21/hf_prune.py#L219.
- [11] 2024. MeetingBank compressed. <https://huggingface.co/datasets/microsoft/MeetingBank-LLMCompressed>.
- [12] 2024. mllm. <https://github.com/UbiquitousLearning/mllm>.
- [13] 2024. redmi-k60-champion-edition. <https://www.giztop.com/redmi-k60-champion-edition.html>.
- [14] 2024. Redmi K70 Pro. <https://www.mi.com/redmi-k70-pro>.
- [15] 2024. rewind. <https://www.rewind.ai/>.
- [16] 2024. XiaoAi smart assistant. <https://xiaoi.mi.com/>.
- [17] 2024. xiaomi-14. <https://www.mi.com/global/product/xiaomi-14/>.
- [18] OpenAI: Josh Achiam, Steven Adler, Sandhini Agarwal, Lama Ahmad, Ilge Akkaya, et al. 2023. GPT-4 Technical Report. arXiv:2303.08774 [cs.CL]
- [19] Abien Fred Agarap. 2019. Deep Learning using Rectified Linear Units (ReLU). arXiv:1803.08375 [cs.NE] <https://arxiv.org/abs/1803.08375>
- [20] Jinze Bai, Shuai Bai, Yunfei Chu, Zeyu Cui, Kai Dang, Xiaodong Deng, Yang Fan, et al. 2023. Qwen Technical Report. arXiv preprint arXiv:2309.16609 (2023).
- [21] Han Cai, Chuang Gan, Tianzhe Wang, Zhekai Zhang, and Song Han. 2020. Once-for-All: Train One Network and Specialize it for Efficient Deployment. arXiv:1908.09791 [cs.LG] <https://arxiv.org/abs/1908.09791>
- [22] Shijie Cao, Lingxiao Ma, Wencong Xiao, Chen Zhang, Yunxin Liu, Lintao Zhang, Lanshun Nie, and Zhi Yang. 2019. SeerNet: Predicting Convolutional Neural Network Feature-Map Sparsity Through Low-Bit Quantization. In *2019 IEEE/CVF Conference on Computer Vision and Pattern Recognition (CVPR)*. 11208–11217. <https://doi.org/10.1109/CVPR.2019.01147>
- [23] Wei Chen and Zhiyuan Li. 2024. Octopus v2: On-device language model for super agent. arXiv:2404.01744 [cs.CL]
- [24] Peter Clark, Isaac Cowhey, Oren Etzioni, Tushar Khot, Ashish Sabharwal, Carissa Schoenick, and Oyvind Tafjord. 2018. Think you have Solved Question Answering? Try ARC, the AI2 Reasoning Challenge. arXiv:1803.05457v1 (2018).
- [25] Jacob Devlin, Ming-Wei Chang, Kenton Lee, and Kristina Toutanova. 2019. BERT: Pre-training of Deep Bidirectional Transformers for Language Understanding. arXiv:1810.04805 [cs.CL] <https://arxiv.org/abs/1810.04805>
- [26] Qingxiu Dong, Lei Li, Damai Dai, Ce Zheng, Jingyuan Ma, Rui Li, Heming Xia, Jingjing Xu, Zhiyong Wu, Baobao Chang, Xu Sun, Lei Li, and Zhifang Sui. 2024. A Survey on In-context Learning. arXiv:2301.00234 [cs.CL] <https://arxiv.org/abs/2301.00234>
- [27] Abhimanyu Dubey, Abhinav Jauhri, et al. 2024. The Llama 3 Herd of Models. arXiv:2407.21783 [cs.AI] <https://arxiv.org/abs/2407.21783>
- [28] Biyi Fang, Xiao Zeng, and Mi Zhang. 2018. NestDNN: Resource-Aware Multi-Tenant On-Device Deep Learning for Continuous Mobile Vision. In *Proceedings of the 24th Annual International Conference on Mobile Computing and Networking (MobiCom ’18)*. ACM. <https://doi.org/10.1145/3241539.3241559>
- [29] Gongfan Fang, Xinyin Ma, Mingli Song, Michael Bi Mi, and Xinchao Wang. 2023. Depgraph: Towards any structural pruning. In *Proceedings of the IEEE/CVF Conference on Computer Vision and Pattern Recognition*. 16091–16101.
- [30] Yingqiang Ge, Yujie Ren, Wenyue Hua, Shuyuan Xu, Juntao Tan, and Yongfeng Zhang. 2023. LLM as OS, Agents as Apps: Envisioning AIOS, Agents and the AIOS-Agent Ecosystem. arXiv:2312.03815 [cs.OS] <https://arxiv.org/abs/2312.03815>
- [31] Rui Han, Qinglong Zhang, Chi Harold Liu, Guoren Wang, Jian Tang, and Lydia Y. Chen. 2021. LegoDNN: block-grained scaling of deep neural networks for mobile vision. In *Proceedings of the 27th Annual International Conference on Mobile Computing and Networking (ACM MobiCom ’21)*. ACM. <https://doi.org/10.1145/3447993.3483249>
- [32] Song Han, Jeff Pool, John Tran, and William J. Dally. 2015. Learning both Weights and Connections for Efficient Neural Networks. arXiv:1506.02626 [cs.NE] <https://arxiv.org/abs/1506.02626>
- [33] Dan Hendrycks, Collin Burns, Steven Basart, Andy Zou, Mantas Mazeika, Dawn Song, and Jacob Steinhardt. 2021. Measuring Massive Multitask Language Understanding. *Proceedings of the International Conference on Learning Representations (ICLR)* (2021).
- [34] Edward J. Hu, Yelong Shen, Phillip Wallis, Zeyuan Allen-Zhu, Yanzhi Li, Shean Wang, Lu Wang, and Weizhu Chen. 2021. LoRA: Low-Rank Adaptation of Large Language Models. arXiv:2106.09685 [cs.CL] <https://arxiv.org/abs/2106.09685>
- [35] Kai Huang, Boyuan Yang, and Wei Gao. 2023. ElasticTrainer: Speeding Up On-Device Training with Runtime Elastic Tensor Selection. In

- Proceedings of the 21st Annual International Conference on Mobile Systems, Applications and Services. 56–69.
- [36] Steven A. Janowsky. 1989. Pruning versus clipping in neural networks. *Phys. Rev. A* 39 (Jun 1989), 6600–6603. Issue 12. <https://doi.org/10.1103/PhysRevA.39.6600>
- [37] Huiqiang Jiang, Qianhui Wu, Chin-Yew Lin, Yuqing Yang, and Lili Qiu. 2023. LLMingua: Compressing Prompts for Accelerated Inference of Large Language Models. *arXiv:2310.05736 [cs.CL]* <https://arxiv.org/abs/2310.05736>
- [38] Huiqiang Jiang, Qianhui Wu, Xufang Luo, Dongsheng Li, Chin-Yew Lin, Yuqing Yang, and Lili Qiu. 2024. LongLLMingua: Accelerating and Enhancing LLMs in Long Context Scenarios via Prompt Compression. In *Proceedings of the 62nd Annual Meeting of the Association for Computational Linguistics (Volume 1: Long Papers)*, Lun-Wei Ku, Andre Martins, and Vivek Srikumar (Eds.). Association for Computational Linguistics, Bangkok, Thailand, 1658–1677. <https://aclanthology.org/2024.acl-long.91>
- [39] Xiaotang Jiang, Huan Wang, Yiliu Chen, Ziqi Wu, Lichuan Wang, Bin Zou, Yafeng Yang, Zongyang Cui, Yu Cai, Tianhang Yu, Chengfei Lv, and Zhihua Wu. 2020. MNN: A Universal and Efficient Inference Engine. In *MLSys*.
- [40] Rui Kong, Yuanchun Li, Yizhen Yuan, and Linghe Kong. 2023. ConvReLU++: Reference-based Lossless Acceleration of Conv-ReLU Operations on Mobile CPU (MobiSys '23). Association for Computing Machinery, New York, NY, USA, 503–515. <https://doi.org/10.1145/3581791.3596831>
- [41] Woosuk Kwon, Zhuohan Li, Siyuan Zhuang, Ying Sheng, Lianmin Zheng, Cody Hao Yu, Joseph E. Gonzalez, Hao Zhang, and Ion Stoica. 2023. Efficient Memory Management for Large Language Model Serving with PagedAttention. *arXiv:2309.06180 [cs.LG]* <https://arxiv.org/abs/2309.06180>
- [42] Ang Li, Jingwei Sun, Pengcheng Li, Yu Pu, Hai Li, and Yiran Chen. 2021. Hermes: an efficient federated learning framework for heterogeneous mobile clients. In *Proceedings of the 27th Annual International Conference on Mobile Computing and Networking (New Orleans, Louisiana) (MobiCom '21)*. Association for Computing Machinery, New York, NY, USA, 420–437. <https://doi.org/10.1145/3447993.3483278>
- [43] Hao Li, Asim Kadav, Igor Durdanovic, Hanan Samet, and Hans Peter Graf. 2017. Pruning Filters for Efficient ConvNets. *arXiv:1608.08710 [cs.CV]* <https://arxiv.org/abs/1608.08710>
- [44] Yuanchun Li, Hao Wen, Weijun Wang, Xiangyu Li, Yizhen Yuan, Guohong Liu, Jiacheng Liu, Wenxing Xu, Xiang Wang, Yi Sun, Rui Kong, Yile Wang, Hanfei Geng, Jian Luan, Xuefeng Jin, Zilong Ye, Guanqing Xiong, Fan Zhang, Xiang Li, Mengwei Xu, Zhiyun Li, Peng Li, Yang Liu, Ya-Qin Zhang, and Yunxin Liu. 2024. Personal LLM Agents: Insights and Survey about the Capability, Efficiency and Security. *arXiv preprint arXiv:2401.05459* (2024).
- [45] Zichang Liu, Jue Wang, Tri Dao, Tianyi Zhou, Binhang Yuan, Zhao Song, Anshumali Shrivastava, Ce Zhang, Yuandong Tian, Christopher Re, and Beidi Chen. 2023. Deja Vu: Contextual Sparsity for Efficient LLMs at Inference Time. In *Proceedings of the 40th International Conference on Machine Learning (Proceedings of Machine Learning Research, Vol. 202)*, Andreas Krause, Emma Brunskill, Kyunghyun Cho, Barbara Engelhardt, Sivan Sabato, and Jonathan Scarlett (Eds.). PMLR, 22137–22176. <https://proceedings.mlr.press/v202/liu23am.html>
- [46] Xinyin Ma, Gongfan Wang, and Xinchao Wang. 2023. LLM-Pruner: On the Structural Pruning of Large Language Models. In *Advances in Neural Information Processing Systems*.
- [47] Kai Mei, Zelong Li, Shuyuan Xu, Ruosong Ye, Yingqiang Ge, and Yongfeng Zhang. 2024. AIOS: LLM Agent Operating System. *arXiv:2403.16971 [cs.OS]* <https://arxiv.org/abs/2403.16971>
- [48] Xupeng Miao, Gabriele Oliaro, Zhihao Zhang, Xinhao Cheng, Zeyu Wang, Zhengxin Zhang, Rae Ying Yee Wong, Alan Zhu, Lijie Yang, Xiaoxiang Shi, Chunan Shi, Zhuoming Chen, Daiyaan Arfeen, Reyna Abhyankar, and Zhihao Jia. 2024. SpecInfer: Accelerating Large Language Model Serving with Tree-based Speculative Inference and Verification. In *Proceedings of the 29th ACM International Conference on Architectural Support for Programming Languages and Operating Systems, Volume 3 (ASPLOS '24)*. ACM. <https://doi.org/10.1145/3620666.3651335>
- [49] Todor Mihaylov, Peter Clark, Tushar Khot, and Ashish Sabharwal. 2018. Can a Suit of Armor Conduct Electricity? A New Dataset for Open Book Question Answering. In *EMNLP*.
- [50] Ali Modarressi, Hosein Mohebbi, and Mohammad Taher Pilehvar. 2022. AdapLeR: Speeding up Inference by Adaptive Length Reduction. In *Proceedings of the 60th Annual Meeting of the Association for Computational Linguistics (Volume 1: Long Papers)*, Smaranda Muresan, Preslav Nakov, and Aline Villavicencio (Eds.). Association for Computational Linguistics, Dublin, Ireland, 1–15. <https://doi.org/10.18653/v1/2022.acl-long.1>
- [51] Subhabrata Mukherjee, Arindam Mitra, Ganesh Jawahar, Sahaj Agarwal, Hamid Palangi, and Ahmed Awadallah. 2023. Orca: Progressive Learning from Complex Explanation Traces of GPT-4. *arXiv:2306.02707 [cs.CL]*
- [52] Long Ouyang, Jeff Wu, Xu Jiang, Diogo Almeida, Carroll L. Wainwright, Pamela Mishkin, Chong Zhang, Sandhini Agarwal, Katarina Slama, Alex Ray, John Schulman, Jacob Hilton, Fraser Kelton, Luke Miller, Maddie Simens, Amanda Askell, Peter Welinder, Paul Christiano, Jan Leike, and Ryan Lowe. 2022. Training language models to follow instructions with human feedback. *arXiv:2203.02155 [cs.CL]* <https://arxiv.org/abs/2203.02155>
- [53] Charles Packer, Sarah Wooders, Kevin Lin, Vivian Fang, Shishir G. Patil, Ion Stoica, and Joseph E. Gonzalez. 2024. MemGPT: Towards LLMs as Operating Systems. *arXiv:2310.08560 [cs.AI]* <https://arxiv.org/abs/2310.08560>
- [54] Zhuoshi Pan, Qianhui Wu, Huiqiang Jiang, Menglin Xia, Xufang Luo, Jue Zhang, Qingwei Lin, Victor Ruhle, Yuqing Yang, Chin-Yew Lin, H. Vicky Zhao, Lili Qiu, and Dongmei Zhang. 2024. LLMingua-2: Data Distillation for Efficient and Faithful Task-Agnostic Prompt Compression. *ArXiv preprint abs/2403.12968* (2024). <https://arxiv.org/abs/2403.12968>
- [55] Adam Paszke, Sam Gross, Francisco Massa, et al. 2019. PyTorch: An Imperative Style, High-Performance Deep Learning Library. *arXiv:1912.01703 [cs.LG]* <https://arxiv.org/abs/1912.01703>
- [56] Colin Raffel, Noam Shazeer, Adam Roberts, Katherine Lee, Sharan Narang, Michael Matena, Yanqi Zhou, Wei Li, and Peter J. Liu. 2023. Exploring the Limits of Transfer Learning with a Unified Text-to-Text Transformer. *arXiv:1910.10683 [cs.LG]* <https://arxiv.org/abs/1910.10683>
- [57] Ramprasaath R. Selvaraju, Michael Cogswell, Abhishek Das, Ramakrishna Vedantam, Devi Parikh, and Dhruv Batra. 2019. Grad-CAM: Visual Explanations from Deep Networks via Gradient-Based Localization. *International Journal of Computer Vision* 128, 2 (Oct. 2019), 336–359. <https://doi.org/10.1007/s11263-019-01228-7>
- [58] Yixin Song, Zeyu Mi, Haotong Xie, and Haibo Chen. 2023. PowerInfer: Fast Large Language Model Serving with a Consumer-grade GPU. *arXiv:2312.12456 [cs.LG]*
- [59] Jianlin Su, Yu Lu, Shengfeng Pan, Ahmed Murtadha, Bo Wen, and Yunfeng Liu. 2023. RoFormer: Enhanced Transformer with Rotary Position Embedding. *arXiv:2104.09864 [cs.CL]* <https://arxiv.org/abs/2104.09864>
- [60] Mingjie Sun, Zhuang Liu, Anna Bair, and J. Zico Kolter. 2024. A Simple and Effective Pruning Approach for Large Language Models.

- arXiv:2306.11695 [cs.CL] <https://arxiv.org/abs/2306.11695>
- [61] Zhiqing Sun, Hongkun Yu, Xiaodan Song, Renjie Liu, Yiming Yang, and Denny Zhou. 2020. MobileBERT: a Compact Task-Agnostic BERT for Resource-Limited Devices. arXiv:2004.02984 [cs.CL] <https://arxiv.org/abs/2004.02984>
- [62] Mukund Sundararajan, Ankur Taly, and Qiqi Yan. 2017. Axiomatic Attribution for Deep Networks. arXiv:1703.01365 [cs.LG] <https://arxiv.org/abs/1703.01365>
- [63] Earl William Swokowski. 1979. *Calculus with analytic geometry*. Taylor & Francis.
- [64] Thierry Tambe, Coleman Hooper, Lillian Pentecost, Tianyu Jia, En-Yu Yang, Marco Donato, Victor Sanh, Paul N. Whatmough, Alexander M. Rush, David Brooks, and Gu-Yeon Wei. 2021. EdgeBERT: Sentence-Level Energy Optimizations for Latency-Aware Multi-Task NLP Inference. arXiv:2011.14203 [cs.AR] <https://arxiv.org/abs/2011.14203>
- [65] Rohan Taori, Ishaan Gulrajani, Tianyi Zhang, Yann Dubois, Xuechen Li, Carlos Guestrin, Percy Liang, and Tatsunori B. Hashimoto. 2023. Stanford Alpaca: An Instruction-following LLaMA model. https://github.com/tatsu-lab/stanford_alpaca.
- [66] MLC team. 2023. *MLC-LLM*. <https://github.com/mlc-ai/mlc-llm>
- [67] Surat Teerapittayanon, Bradley McDanel, and H. T. Kung. 2017. BranchyNet: Fast Inference via Early Exiting from Deep Neural Networks. arXiv:1709.01686 [cs.NE] <https://arxiv.org/abs/1709.01686>
- [68] Hugo Touvron, Thibaut Lavril, Gautier Izacard, Xavier Martinet, Marie-Anne Lachaux, Timothée Lacroix, Baptiste Rozière, Naman Goyal, Eric Hambro, Faisal Azhar, Aurelien Rodriguez, Armand Joulin, Edouard Grave, and Guillaume Lample. 2023. LLaMA: Open and Efficient Foundation Language Models. arXiv:2302.13971 [cs.CL] <https://arxiv.org/abs/2302.13971>
- [69] Alex Wang, Amanpreet Singh, Julian Michael, Felix Hill, Omer Levy, and Samuel R. Bowman. 2019. GLUE: A Multi-Task Benchmark and Analysis Platform for Natural Language Understanding. arXiv:1804.07461 [cs.CL] <https://arxiv.org/abs/1804.07461>
- [70] Yubo Wang, Xueguang Ma, et al. 2024. MMLU-Pro: A More Robust and Challenging Multi-Task Language Understanding Benchmark. arXiv:2406.01574 [cs.CL] <https://arxiv.org/abs/2406.01574>
- [71] Hao Wen, Yuanchun Li, Guohong Liu, Shanhui Zhao, Tao Yu, Toby Jia-Jun Li, Shiqi Jiang, Yunhao Liu, Yaqin Zhang, and Yunxin Liu. 2024. AutoDroid: LLM-powered Task Automation in Android. In *Proceedings of the 30th Annual International Conference on Mobile Computing and Networking* (Washington D.C., DC, USA) (ACM MobiCom '24). Association for Computing Machinery, New York, NY, USA, 543–557. <https://doi.org/10.1145/3636534.3649379>
- [72] Hao Wen, Yuanchun Li, Zunshuai Zhang, Shiqi Jiang, Xiaozhou Ye, Ye Ouyang, Ya-Qin Zhang, and Yunxin Liu. 2023. AdaptiveNet: Post-deployment Neural Architecture Adaptation for Diverse Edge Environments. arXiv:2303.07129 [cs.LG] <https://arxiv.org/abs/2303.07129>
- [73] Noam Wies, Yoav Levine, and Amnon Shashua. 2023. The Learnability of In-Context Learning. arXiv:2303.07895 [cs.CL] <https://arxiv.org/abs/2303.07895>
- [74] Thomas Wolf, Lysandre Debut, Victor Sanh, Julien Chaumond, Clement Delangue, et al. 2020. Transformers: State-of-the-Art Natural Language Processing. In *Proceedings of the 2020 Conference on Empirical Methods in Natural Language Processing: System Demonstrations*. Association for Computational Linguistics, Online, 38–45. <https://www.aclweb.org/anthology/2020.emnlp-demos.6>
- [75] Minghao Wu, Abdul Waheed, Chiyu Zhang, Muhammad Abdul-Mageed, and Alham Fikri Aji. 2023. LaMini-LM: A Diverse Herd of Distilled Models from Large-Scale Instructions. CoRR abs/2304.14402 (2023). arXiv:2304.14402 <https://arxiv.org/abs/2304.14402>
- [76] Mengzhou Xia, Tianyu Gao, Zhiyuan Zeng, and Danqi Chen. 2024. Sheared LLaMA: Accelerating Language Model Pre-training via Structured Pruning. arXiv:2310.06694 [cs.CL] <https://arxiv.org/abs/2310.06694>
- [77] Daliang Xu, Wangsong Yin, Xin Jin, Ying Zhang, Shiyun Wei, Mengwei Xu, and Xuanzhe Liu. 2023. LLMcad: Fast and Scalable On-device Large Language Model Inference. arXiv:2309.04255 [cs.NI] <https://arxiv.org/abs/2309.04255>
- [78] Daliang Xu, Hao Zhang, Liming Yang, Ruiqi Liu, Gang Huang, Mengwei Xu, and Xuanzhe Liu. 2024. Empowering 1000 tokens/second on-device LLM prefilling with mllm-NPU. arXiv:2407.05858 [cs.AI] <https://arxiv.org/abs/2407.05858>
- [79] Mengwei Xu, Wangsong Yin, Dongqi Cai, Rongjie Yi, Daliang Xu, Qipeng Wang, Bingyang Wu, Yihao Zhao, Chen Yang, Shihe Wang, Qiyang Zhang, Zhenyan Lu, Li Zhang, Shangguang Wang, Yuanchun Li, Yunxin Liu, Xin Jin, and Xuanzhe Liu. 2024. A Survey of Resource-efficient LLM and Multimodal Foundation Models. arXiv:2401.08092 [cs.LG] <https://arxiv.org/abs/2401.08092>
- [80] Zhenliang Xue, Yixin Song, Zeyu Mi, Le Chen, Yubin Xia, and Haibo Chen. 2024. PowerInfer-2: Fast Large Language Model Inference on a Smartphone. arXiv:2406.06282 [cs.LG] <https://arxiv.org/abs/2406.06282>
- [81] Rongjie Yi, Liwei Guo, Shiyun Wei, Ao Zhou, Shangguang Wang, and Mengwei Xu. 2023. EdgeMoE: Fast On-Device Inference of MoE-based Large Language Models. arXiv:2308.14352 [cs.LG] <https://arxiv.org/abs/2308.14352>
- [82] Wangsong Yin, Mengwei Xu, Yuanchun Li, and Xuanzhe Liu. 2024. LLM as a System Service on Mobile Devices. arXiv:2403.11805 [cs.OS] <https://arxiv.org/abs/2403.11805>
- [83] Jinliang Yuan, Chen Yang, Dongqi Cai, Shihe Wang, Xin Yuan, Zeling Zhang, Xiang Li, Dingge Zhang, Hanzi Mei, Xianqing Jia, Shangguang Wang, and Mengwei Xu. 2024. Mobile Foundation Model as Firmware. In *Proceedings of the 30th Annual International Conference on Mobile Computing and Networking* (Washington D.C., DC, USA) (ACM MobiCom '24). Association for Computing Machinery, New York, NY, USA, 279–295. <https://doi.org/10.1145/3636534.3649361>
- [84] Li Zhang, Shihe Wang, Xianqing Jia, Zhihan Zheng, Yunhe Yan, Longxi Gao, Yuanchun Li, and Mengwei Xu. 2024. LlamaTouch: A Faithful and Scalable Testbed for Mobile UI Task Automation. arXiv:2404.16054 [cs.HC] <https://arxiv.org/abs/2404.16054>
- [85] Susan Zhang, Stephen Roller, et al. 2022. OPT: Open Pre-trained Transformer Language Models. arXiv:2205.01068 [cs.CL] <https://arxiv.org/abs/2205.01068>
- [86] Lianmin Zheng, Wei-Lin Chiang, Ying Sheng, Siyuan Zhuang, Zhanghao Wu, Yonghao Zhuang, Zi Lin, Zhuohan Li, Dacheng Li, Eric P Xing, Hao Zhang, Joseph E. Gonzalez, and Ion Stoica. 2023. Judging LLM-as-a-judge with MT-Bench and Chatbot Arena. arXiv:2306.05685 [cs.CL]
- [87] Ningxin Zheng, Huiqiang Jiang, Quanlu Zhang, Zhenhua Han, Lingxiao Ma, Yuqing Yang, Fan Yang, Chengruidong Zhang, Lili Qiu, Mao Yang, and Lidong Zhou. 2023. PIT: Optimization of Dynamic Sparse Deep Learning Models via Permutation Invariant Transformation. In *Proceedings of the 29th Symposium on Operating Systems Principles* (Koblenz, Germany) (SOSP '23). Association for Computing Machinery, New York, NY, USA, 331–347. <https://doi.org/10.1145/3600006.3613139>
- [88] Jeffrey Zhou, Tianjian Lu, Swaroop Mishra, Siddhartha Brahma, Sujoy Basu, Yi Luan, Denny Zhou, and Le Hou. 2023. Instruction-Following Evaluation for Large Language Models. arXiv:2311.07911 [cs.CL] <https://arxiv.org/abs/2311.07911>
- [89] Yukun Zhu, Ryan Kiros, Rich Zemel, Ruslan Salakhutdinov, Raquel Urtasun, Antonio Torralba, and Sanja Fidler. 2015. Aligning Books and Movies: Towards Story-Like Visual Explanations by Watching Movies and Reading Books. In *The IEEE International Conference on*

Conference'17, July 2017, Washington, DC, USA

Wangsong Yin[◆], Rongjie Yi[◇], Daliang Xu[◆], Gang Huang[◆],
Mengwei Xu[◇], Xuanzhe Liu[◆]

Computer Vision (ICCV).